



DESIGN, CONSTRUCTION AND PERFORMANCE EVALUATION OF A SMALL SCALE BIOFUEL DISTILLER

L. N. Onuoha^{1*}, M. O. I. Nwafor¹, J. O. Igbokwe¹ and N. A. Aviara²

¹Department of Mechanical Engineering, Federal University of Technology Owerri, Imo State, Nigeria

²Department of Agricultural and Environmental Resources Engineering,
University of Maiduguri, Maiduguri, Borno State, Nigeria

*Corresponding author's e-mail address: freshlove2006@gmail.com

ARTICLE INFORMATION

Submitted 6 July, 2018

Revised 10 May, 2019

Accepted 12 June, 2019

Keywords:

Biofuel
Distiller
Biomass
Bioethanol.

ABSTRACT

A biofuel distiller of 20 L feed capacity was designed fabricated and used to distill bioethanol from a biomass broth. The distiller consists of a 40 L volume boiler unit integrated to the combustion chamber as a cylindrical column; and a counter current cylindrical condenser of length, tube and shell internal diameter of 88 cm, 0.0191/0.15 m, inclined at 45°. The reactor is a Top Lit Updraft (T-LUD) type fired with charcoal of moderate lump. Its performance evaluation was conducted using 20 L palm bunch broth as the distiller feed. The palm bunch collected from Siat Nigeria Ltd, Ubima, Rivers State, Nigeria, was physically pretreated by grinding to powder, hydrolyzed with 1.2 % dilute H₂SO₄, at 160°C for 30 min and fermented for 72 h with *S.cerevisiae* separated from palm wine. The broth was then separated from the slurry by filtering before distillation. The result of the machine evaluation showed that 817 ml bioethanol was obtained per batch at 20 min from the bubble point which took 95 min. Actual combustion efficiency was found to be 55 % with reactor power rating of 12.2 kW. The machine vaporized bioethanol fuel from the boiler feed fed at 27°C, and released the distillate at 28.3°C. Distillation efficiency was found to be greater than 90 % while the maximum productivity occurred at 10 min from the bubble point. The machine is economical, reliable, convenient to use and can stand diverse environmental conditions. It can be integrated as a waste management step in the downstream end of palm mill operations.

1.0 Introduction

There is need for biofuels production to augment the use of fossil fuels, and to establish a strong link between the downstream petroleum industry and agricultural activities (NNPC, 2007), especially in developing countries. Consequently, countries are steered towards establishing biofuels industry that is commercially viable to both investors and consumers, and provide sustainable job opportunities that could reach the common man. Biomass wastes are among the feedstock for renewable energy to achieve the requirement of Carbon Emission Reduction (CERs)

credits. Owing to its widespread availability, biorenewable fuel technology will potentially result in the employment of more people than fossil-fuel-based technology (Demirbas, 2006; Shyam et al., 2012; Karl et al., 2005). Palm oil industries which are striving towards quality and environmental conservation through a 'sustainable development and cleaner technology' based on the requirements of Environmental Quality Act (EQA) and the specific regulations governing the management of Palm Oil mills; can then fully comply to regulatory requirements in terms of combustion, fly ash and energy conservation (Yusoff, 2006) by transforming the residue into biofuel 'a more-valuable end product' (Yong et al., 2007) such as waste palm bunch to bioethanol. Efficient implementation of bioethanol production from these wastes can be a breakthrough in the fuel market or world's energy portfolio (Piotr et al., 2008; Leland, 2005). These feedstocks when properly treated can be reduced to biofuel. There is need to separate the pure biofuel from the obtained mixture, and this is mostly achieved by distillation for bioethanol. Distillation is a thermal separation technique relying on differences in the boiling points of the component liquids to be separated (Sudheer, 2013; Smith, 1995). The motive force in all thermal separation is the drive towards thermodynamic equilibrium between the different phases (vapor liquid equilibrium, VLE) (Tongfan et al., 2004). The concentration of the lighter components will be greater in the vapor phase and conversely the concentration of the heavier components will be greater in the liquid phase, and only in the case of pure components or azeotropic mixtures will the equilibrium composition be the same in both phases (Jim, 2005; Smith et al., 2001). Boiling point and vapor pressure are the key parameters and higher vapor pressure creates a lower boiling point. Matherson (1980) noted that when alcohol/water mixture is boiled, vapors with a greater concentration of alcohol forms while liquid with a lesser concentration of alcohol remains behind. Separation of the bioethanol from water is initiated at this stage taking advantage of the low boiling point of bioethanol (78 °C) and the positive azeotrope it forms with water (Jim, 2005). Depending on the availability and cost, different fuels can be used for heating such as fossil fuels: kerosene, diesel, LPG; electricity; or biomass: firewood, charcoal, pellets etc. Biomass or electricity is often used because of their availability, ease of handling and simplicity of design. Biomass combustion equipment is often simpler and cheaper than equipment for other technologies (Sheng and Azevedo, 2005). The potential of biomass as alternative fuel source to replace LPG is a promising option (Hassan et al., 2011). Traditionally, energy in the form of firewood, pellets, twigs and charcoal has been the major source of renewable energy for many developing countries (Emerhi, 2011). Charcoal could be used as a heat source for bioethanol distillation because of its low price and ease of procurement in agricultural countries like Nigeria. A fuel's energy density can depend on its concentration which is the purity, and yield as a basis of economic measure on its viability as related to the process technology adopted (Antonia et al., 2001). Presently, only few industries produce bioethanol fuel partly because of the cost of importing a sophisticated distiller. Also, irrespective of the negative health effect, people have taken to local production of bioethanol for consumption due to the ease of doing this with ordinary pots but in hideouts as it is banned by the government. Therefore introducing an affordable distiller will engage more industries into the biofuel production as well as encourage local producers to produce bioethanol for fuel rather than consumption which has a negative health effect. The main objectives of this study was to fabricate a biofuel distiller that will produce quality bioethanol at low cost. The distiller will be analyzed base on: thermal efficiency, distiller capacity, bioethanol yield, distillation rate, distillation productivity and distillation efficiency.

2.0 Methodology

2.1 Feedstock Collection and Preparation

Palm bunch collected from Siat Nigeria Ltd, Ubima, Rivers State, Nigeria, was reduced to bioethanol broth; by grinding, hydrolysis and fermentation (Nuru et al., 2014; Julia'n et al., 2011). After physical pretreatment, the waste palm bunch was subjected to hydrolysis on condition of 1.2 % dilute H₂SO₄, at 160 °C for 30 min and fermentation for 72 h with *S.scerevisiae* separated from palm wine. Broth was then separated from the slurry by filtering because; distilling the whole slurry will definitely affect clear separation of the fermented portion of the feed and invariably affect the final yield (Olaoye, 2011). Total bioethanol concentration in the broth was estimated by Chromic acid method; and absorbance determined at 584 nm wavelength using a spectrophotometer was converted to bioethanol concentration from a standard curve for standard solution of absolute ethanol (Caputi et al., 1968; Congcong et al., 2013).

2.2 Distiller Design Procedures

The designed distiller is expected to distill bioethanol from a 20 L feed which consists mainly of bioethanol and water. The distiller composes of a boiler, condenser and a coolant storage tank unit. The boiler is the feed holding space where pressure is built in response to increasing temperature due to heat supply from an incorporated reactor. It is also incorporated with a thermometer and pressure gauge for temperature and pressure reading. The condenser condenses bioethanol vapor by extracting heat from it. The coolant storage tank stores the coolant which circulates through the condenser. The following were considered in the design:

- a) Thermal and physical properties of ethanol
- b) Thermal and physical properties of feed and its constituents.
- c) Quantity of feed and bioethanol content to be distilled.
- d) Heat energy requirement
- e) Fuel type and the required quantity.
- f) Properties of fuel and conditions for complete combustion.

In order to accommodate generated vapor, the feed is considered as half of boiler volume. Below the boiler capacity, the rising vapor will lose energy and cool down before it reaches the condenser; as such the yield will be low (Bolling and Suarez, 2001). Charcoal was selected as the reactor fuel because of its low price and ease of procurement. Properties of charcoal depend on its wood specie and specific gasification rate of wood which is in the range of 100 - 250 kg/m²h (Ojolo et al., 2012a). Thus, the heating value of the Charcoal is classified within the range for that of Acacia species residue given by Tarig and Osman (2012) as 17,386 – 19,309 kJ/kg with density range of 226.3 – 728 kg/m³. Stoichiometric air (SA) of charcoal was given as 8.4 m³ air per kg by Engineering Toolbox (2016) while 9.98 kg/kg was given by Baldwin, (1987). Reed (1981) gave its equivalence ratio (e) as 0.25 considering its low carbon content compared to wood. Its specific gasification rate (SGR) ranges from 78 – 86 kg/m²-h (Ojolo et al., 2012b). In the design, the following were considered for charcoal: 19,309 kJ/kg fuel heating value (HVF), 80 kg/m²-h SGR, 230 kg/m³ density and 9.98 kg/kg SA. The charcoal is considerably dry. Updraft reactor is chosen because of its advantages (FAO, 1985) which include;

- (1) ease of operation
- (2) high charcoal burnout

- (3) high equipment efficiency
- (4) possibility of operating with fuel varieties
- (5) high heat transfer.

Its main disadvantage is channeling difficulty which can lead to oxygen breakthrough and consequence explosion; this can be checked by appropriate air current and channel column. Prevailing ambient temperature (T_{amb}) was simulated to be 30 °C while other parameters were calculated from basic formula as outlined below.

2.3 Energy and Fuel Requirement

(a) Energy needed for distillation Q_n is the sum of heat energy required to raise the temperature of the feed from initial temperature to its bubble point that needed to change bioethanol to vapor at the feed bubble point. Q_n is calculated according to Eke (1991) using Equation (1).

$$Q_n = M.C.\Delta\theta + ML \quad (1)$$

where: M is mass of feed in (kg). C is Specific heat of feed (kJ/kg°C). L is latent heat of vaporization of bioethanol at its boiling point (kJ/kg°C). L is chosen at its boiling point because highest energy to convert bioethanol to vapor is achieved at that point (Li et al., 2010; Iguaz and Vírveda, 2007). $\Delta\theta$ is the temperature difference.

As deduced from Jones and Dugan (1998), Kister (1992), Don and Robert (1997) the specific heat of the feed is calculated at its bubble point with Equation (2). Feed bubble point was calculated iteratively at atmospheric pressure to be 99.6 °C.

$$C_{feed} = (C_{eth} \cdot x_{eth}) + (C_w \cdot x_w) \quad (2)$$

where: x and C are liquid mole fraction and specific heat (kJ/kg.K) at bubble point respectively.

The bubble point of the binary feed is the temperature (at a given pressure) at which the first bubble of vapor is formed when heated i.e. the point at which the first drop of a liquid mixture begins to vaporize (Kister, 1992, Don and Robert, 1997). Vapor pressure of the components was calculated with Antoine Constants as given in Equation (3) while Equation (4) gives their vapor mole fraction.

$$\text{Log}_{10}P_{(\text{mmHg})} = A - \frac{B}{C + T} \quad (3)$$

$$\text{Vapor mol fraction} = \frac{(\text{liquid mol fraction})(\text{vapor pressure})}{(\text{atm pressure})} \quad (4)$$

where: A, B, C are Antoine constants corresponding to temperature, T (°C) .

(b) Combustion chamber heat energy input Q_f and boiler power rating p_f were calculated using Equation (5) and (6) respectively, (Theraja et al., 2001):

$$Q_f = Q_n / \text{eff} \quad (5)$$

$$p_f = \frac{Q_f}{3600(\text{sec})} \quad (6)$$

where: eff. is the boiler's calorific efficiency, Q_n is energy needed for distillation (kJ).

(c) Considering 5% loss of heat due to insulating material, total heat energy Q_{Tn} entering the boiler is:

$$Q_{Tn} = Q_n + (\% \text{ loss} \times Q_f) \quad (7)$$

(d) Weight of fuel (charcoal) used WFU (kg) and charcoal consumption rate FCR (kg/hr) were calculated using Equation (8) and (9) respectively (Belonio, 2005):

$$WFU = \frac{Q_f}{HVF} \quad (8)$$

$$FCR = \frac{WFU}{3600} \quad (9)$$

where: HVF is heating value of charcoal (kJ/kg). Normally Q_f may differ from Q_n as it also accounts for heat loss in the boiler unit.

(e) Combustion zone velocity (CZV) was calculated using Equation (10).

$$CZV = \frac{\text{Fuel height}}{\text{Time}} \quad (10)$$

2.3.1 Boiler

Boiler height H_b was determined from Equations (11).

$$H_b = \frac{V_b}{2\pi r^2} \quad (11)$$

where: 'r' is the boiler radius (m) and V_b is boiler volume (m³).

The boiler shell is an alloyed steel cylindrical vessel oriented vertically. The boiler forms a continuous column with the reactor, thus have same shape and diameter. The height of the boiler is moderate for quick even heat distribution in the entire content and πr^2 is heating surface area of the boiler shell.

2.3.2 Reactor

The reactor consists of the combustion chamber and ash chamber. To ensure complete combustion, air cavity of 5.69 cm diameter is considered to run through the combustion chamber (Belonio, 2005). A height of 12 cm was allowed for feeding charcoal into the reactor. Combustion chamber has a mesh floor of 0.25 inches diameter air holes. Ash collection chamber of 32 cm height which carries the fan casing is incorporated to the combustion chamber. The ash chamber has 18 cm clearance from the floor. The reactor diameter was computed according to Belonio (2005) using Equation (12).

$$\text{Reactor diameter, } D = \left(\frac{1.27 \text{ FCR}}{\text{SGR}} \right)^{0.5} \quad (12)$$

The height of the reactor was computed using Equation (13) according to Singh (2008).

$$\text{Reactor height, } H = \frac{\text{SGR} \times T}{\rho_{ch}} \quad (13)$$

where: FCR is fuel consumption rate (kg/s), SGR is specific gasification rate (kg/h.m²), T is time to consume charcoal (h) and ρ_{ch} - charcoal density kg/m³.

Reactor height determines how long the distiller would be operated in one loading of fuel. The higher the reactor, however, the more pressure draft is needed to overcome the resistance exerted by the fan or blower. Inferring from the volume equations, the volume of a reactor defines the quantity of heat that can be released in the combustion chamber (Somchart et al., 2010). The volume of the cylindrical reactor, V_r was calculated using Equation (14)

$$V_r = \pi r^2 h \quad (14)$$

where: h is reactor height (m). Reactor Cross sectional area (CSA) was computed using Equation (15) due to Rathore et al., (2009).

$$CSA = \frac{FCR}{SGR} \quad (15)$$

where: FCR is fuel consumption rate (kg/s) and SGR is specific gasification rate (kg/h.m²).

The ash chamber serves as the discharging unit for ash produced after each operation. It was located beneath the reactor to easily catch the ash that is falling from the reactor. It was always kept closed when operating the distiller. Four metal support legs are provided beneath the ash chamber to support the entire combustion chamber. A chimney was introduced to the reactor top base to allow smoke to pass out.

2.3.3 Computation of Reactor Airflow Rate

Airflow rate, AFR in the reactor was calculated using Equation (16) due to Belonio (2005).

$$AFR = \frac{FCR \times SA}{\rho_{air}} \quad (16)$$

where: FCR is fuel consumption rate (kg/s), SA is stoichiometric air and ρ_{air} is air density.

Superficial velocity, V_s in fuel bed was given by Equation (17) due to Srinivasa et al., (2016).

$$V_s = \frac{AFR}{\text{Reactor area}} \quad (17)$$

where: AFR is airflow rate (m³/s).

This refers to the speed of the air flow in the fuel bed. The velocity of air in the charcoal bed will cause channel formation, which affects combustion. Similarly, the thicker the layer of fuel in the reactor, the greater is the resistance required for the air to pass through the fuel column (Belonio, 2005).

Specific pressure draft of charcoal Δp_w was derived from expression for Total pressure draft given in Equation (18) according to Belonio (2005).

$$P_d = H \times \Delta P \quad (18)$$

where: P_d is the total pressure draft of charcoal (Pa), H is Reactor height (m) and Δp is the corresponding specific pressure draft of charcoal in centimeter of water per meter depth of fuel at the calculated superficial gas velocities.

Considering the work of Bello et al., (2015), Joseph and Oliver (2016), Wusana et al., (2014), Klavina et al., (2014); the pressure drop of charcoal with particle size greater than 6.7 mm is within the range of 30 – 36 Pa for AFR of 0.103 – 115 m/s having a specific air resistance of the range 83 – 102.4 Pa/m. A total pressure drop of 30 Pa was considered for this design. Charcoal does not have severe air resistance and the column is not too high at 0.35m; so, to save cost natural air convection instead of a blower was utilized. In order to meet the furnace requirement of supplying the air flow rate while overcoming the fuel (charcoal) pressure drop; the furnace is constructed with a perforated column (air cavity) attach to its mesh floor, the fan chamber is rather vented and positioned towards the natural air current. The perforated column and floor help to remove ash.

2.3.4 Condenser

The condenser is designed for counter current fluid flow in order to extract a higher proportion of heat from the hot fluid. It is cylindrical and inclined at angle 45° to the boiler column to

ensure slow vapor velocity and achieve complete condensation. The distillation tube is ½" Nominal 'D' copper tube with 0.0205 m OD, 0.01905 m ID, 2.8506 x 10⁻⁴m² CSA and negligible thickness of 0.001 m. Velocity, V_t of bioethanol vapor in the tube and its Reynold's number at the tube inlet condition were calculated using Equation (19) and (20) respectively and found to be laminar with low velocity.

$$V_t = \frac{\dot{V}_{bio}}{CSA_{tube}} \quad (19)$$

$$Re_{vapor} = \frac{\rho_v V_v D}{\mu_v} \quad (20)$$

where: V_t is bioethanol vapour velocity (m/s) in the tube, \dot{V}_{bio} is volumetric velocity of bioethanol (m³/s), CSA_{tube} is tube cross sectional area, D is tube diameter, ρ_v , V_v, μ_v are bioethanol vapour density (kg/m³), velocity (m/s) and viscosity (kg/m.s) respectively.

Thus, the condensation heat transfer coefficient, h_{cond}. was calculated according to Yunus and Afshin (2015) and considering inclination angle using Equation (21).

$$h_{cond} = 0.555 \left[\frac{g \rho_L (\rho_L - \rho_v) K_L^3}{\mu_L (T_{sat} - T_s) D} h_{fg}^* \right]^{1/4} (\sin \theta)^{1/4} \quad (21)$$

And the modified latent heat of vaporization is calculated using Equation (22) according to Yunus and Afshin (2015).

$$h_{fg}^* = h_{fg} + \frac{3}{8} C_{pL} (T_{sat} - T_s) \quad (22)$$

where: ρ , μ , K, C_p and h_{fg} are density (kg/m³), viscosity (kg/m.s), conductivity (W/m.k), specific heat capacity (kJ/kg.K) and latent heat of vaporization (kJ/kg) of the saturated bioethanol while subscripts L and v are for liquid and vapor respectively. T_{sat} and T_s are saturation temperature of bioethanol and tube surface temperature respectively. g is acceleration due to gravity.

The log mean temperature difference, LMTD for the counter current flow heat exchanger is calculated using Equation (23) according to Khurmi and Gupta (2006). Coolant inlet temperature was 30 °C and the required out flow temperature was 40 °C.

$$LMTD = \frac{(T_{h1} - T_{c2}) - (T_{h2} - T_{c1})}{\ln \frac{(T_{h1} - T_{c2})}{(T_{h2} - T_{c1})}} \quad (23)$$

where: T is temperature (°C) and subscripts h, c, 1 and 2 are for hot fluid (bioethanol), cold fluid (coolant), inlet and outlet respectively.

The condenser shell is cylindrical mild steel material of 15 cm diameter and 3 mm thickness with 0.01482 m² cross sectional area (CSA). The quantity of coolant (water) was determined using Equation (24) due to Yunus and Afshin (2015).

$$m_w = \frac{m_{bio} h_{fg}^*}{C_w (T_{c2} - T_{c1})} \quad (24)$$

where: m_{bio}, m_w and C_w are mass of bioethanol (kg), mass (kg) and specific heat (kJ/kg.K) of water respectively. h_{fg}^{*} is the modified latent heat of vaporization (kJ/kg), T_{c2} and T_{c1} are outlet and inlet temperature (°C) of coolant respectively.

Though a cylindrical drum was used to hold coolant and connected to the shell with pipes. A centrifugal pump of 0.5 HP was used to circulate coolant. Velocity of coolant in the shell V_s and

its Reynold's number were calculated using Equation (25) and (26) respectively and found to be laminar with low velocity.

$$V_s = \frac{4 \dot{V}_w}{\pi (D_h)^2} \quad (25)$$

$$R_{e,w} = \frac{\rho V_s D_h}{\mu_s} \quad (26)$$

where: D_h is annulus hydraulic diameter ($ID_{shell} - OD_{tube}$), \dot{V}_w is water velocity (m/s), ρ , V_s and μ_s are density (kg/m^3), velocity (m/s) and viscosity ($kg/m.s$), of shell side fluid.

The tube and shell formed an annulus. The shell-side heat transfer coefficient was calculated using Equation (27).

$$h_{shell} = \frac{Nu_i K}{D_h} \quad (27)$$

where: Nu_i is Nusselt number on the tube of the shell space corresponding to the ratio of the inner and outer diameter of the annulus (OD_{tube}/ID_{shell}). K is conductivity ($W/m.k$), D_h is annulus hydraulic diameter (m). The corresponding Nusselt number was determined from Kay and Perkins (1972). The overall heat transfer coefficient 'U' was calculated using Equation (28) due to Yunus and Afshin (2015).

$$\frac{1}{U} = \frac{1}{h_{cond}} + \frac{1}{h_{shell}} + R_{ft} + R_{fs} \quad (28)$$

where: R_{ft} and R_{fs} are tube-side and shell-side fouling factor due to alcohol and water which by Tubular Exchange Manufacturing Association are 0.0001 each. h_{cond} and h_{shell} are condensation heat transfer coefficient and shell-side heat transfer coefficient respectively ($W/m^2.K$).

Condensation heat transfer surface area A_{total} was calculated using Equation (29).

$$A_{total} = \frac{\dot{Q}}{U.F.LMTD} \quad (29)$$

where: F is correction factor which is '1' for counter flow (Yunus and Afshin, 2015), \dot{Q} is rate of heat transfer, U is overall heat transfer coefficient ($W/m^2.K$), $LMTD$ is log mean temperature difference ($^{\circ}C$).

Length of condenser tube was calculated using Equation (30).

$$L = \frac{A_{total}}{\pi D} \quad (30)$$

where: A_{total} is condensation heat transfer surface area (m^2), D is the tube diameter (m).

Pressure Drop at shell-side was calculated using Equation (31) due to Yunus and Afshin (2015).

$$\Delta P = \frac{32 \mu L V_{avg}}{D_h^2} \quad (31)$$

where: D_h is annulus hydraulic diameter (m), L is shell length (m), V_{avg} is average velocity (m/s) and μ is viscosity at shell side ($kg/m.s$).

Head loss at shell-side was calculated using Equation (32).

$$h_L = \frac{64 L V_{avg}^2}{2 g D_h^2 Re_w} \quad (32)$$

where: D_h is annulus hydraulic diameter (m), L is shell length (m), V_{avg} is average velocity (m/s) and g is acceleration due to gravity, Re_w is Renault number of shell fluid. The head loss is the additional height the fluid needed to be raised by a pump in order to overcome the frictional losses in the shell (Frank and David, 2002).

Pressure loss at shell-side was calculated using Equation (33) due to Yunus and Afshin (2015).

$$\Delta P_L = \rho g [h_L - L \sin 45^\circ] \quad (33)$$

where: h_L is head loss at shell-side (m), ρ is density (kg/m^3), g is acceleration due to gravity, L is shell length (m).

Shell-side pumping power was calculated using Equation (34).

$$W_{\text{pump}} = m g h_L \quad (34)$$

where: h_L is head loss at shell-side (m), m is mass of coolant (kg), g is acceleration due to gravity.

2.4 Distiller Evaluation

The distiller was investigated on average of three distillation runs base on thermal efficiency, distiller capacity, distillation yield, distillation rate, bioethanol productivity and distillation efficiency.

(a) Thermal Efficiency: this is the thermal efficiency of the boiler. It is the ratio of heat actually used in producing the fuel to the heat liberated in the furnace (Khurmi and Gupta, 2006) and is calculated using Equation (35).

$$\eta_{th} = \frac{\text{heat used to produce fuel}}{\text{heat liberated in furnance}} \times 100 \quad (35)$$

(b) Distiller Capacity: this is the power of the constructed distillation unit (Khurmi and Gupta, 2006); it is the amount of bioethanol evaporated or bioethanol fuel (condensate) produced in kg expressed per fuel (kg) burnt using Equation (36).

$$D_c = \frac{m_{eth}}{\text{weigh of fuel burnt}} \quad (36)$$

(c) Distillation Yield: This is alcohol obtained with distillation time (Tangka et al., 2011; Nurul et al., 2014) as expressed in Equation (37). It shows the presence or absent of regression in the distillation process which depends on steadiness of heat supply and heat source sufficiency (Olaoye, 2011).

$$\text{bioethanol fuel yeild (l/min)} = \frac{Q_{be}(l)}{\text{time, } \Delta t} \quad (37)$$

where: Q_{be} bioethanol fuel produced in liters,

(e) Distillation Rate: This is alcohol that could be obtained per hour of distillation process (Will, 2018) as expressed in Equation (38). It shows the speed of the production process.

$$\text{bioethanol fuel yeild (l/h)} = \frac{Q_{be}(l)}{\text{hour (h)}} \quad (38)$$

(f) Bioethanol Productivity: This is bioethanol per minute to volume of feed (Tangka et al., 2011; Nurul et al., 2014) as in Equation (39).

$$\text{bioethanol productivity} = \frac{Q_{be}(\text{l/min})}{\text{feed volume (l)}} \quad (39)$$

(g) Distillation Efficiency: It is a measure of how much alcohol was finally produced relative to the amount that was in the feed. It shows the amount of losses in the evaporation and distillation process (combined Sugar news, 23 July 2016). Distillation efficiency is expressed in Equation (40) by Sugar news (2016).

$$\text{distillation efficiency (\%)} = \frac{\text{vol.of distillate}}{\text{bioethanol content in feed (L)}} \times 100 \quad (40)$$

(h) Other parameters investigated and compared to the designed parameters in a tabular form are fuel weight, boiling point, total operating time, fuel consumption rate, specific gasification rate, combustion zone velocity, reactor power input, bioethanol yield, distillation temperature and vapor pressure.

2.5 Material Selection

Material selection was based on strength/fatigue resistance, heat resistance, wear and corrosion resistance, cost, workability and appearance (Baqui et al., 2008). Appropriate selection of the best materials was ensured to enable the best quality of the distillery unit and bioethanol quality, and to meet design standards. Thus, copper tube was used as the condenser tube (Kris, 2004), alloy steel was used for the shell and boiler unit while glass container collects the distillate (Yuelei et al., 2012). Fiber glass was chosen for insulation of the heating unit. The exploded and isomeric view of the designed equipment is presented in Figure 1 and 2 respectively while Figure 3 is the pictorial view of the fabricated and assembled distiller.

2.6 Fabrication Process

The fabrication steps involved selection and/or cutting of metal sheets into desired sizes, and arc welding joints where necessary to ensure toughness and strength. Parts were welded perfectly with firm joints to avoid vapor loss. Pipe settings were carried out with utmost carefulness. It was subjected to hydrostatic pressure test. Hand pump was use to fill in the shell with water and by pressurizing to set pressure, say 4 or 6 bars. Dye penetration test was done on welded edges to ensure there are no pin holes and cracks on the weld. The pressure was observed for about 25 minutes to ascertain if there were leakages on the tube. The exchanger was then boxed-up and made ready for use.

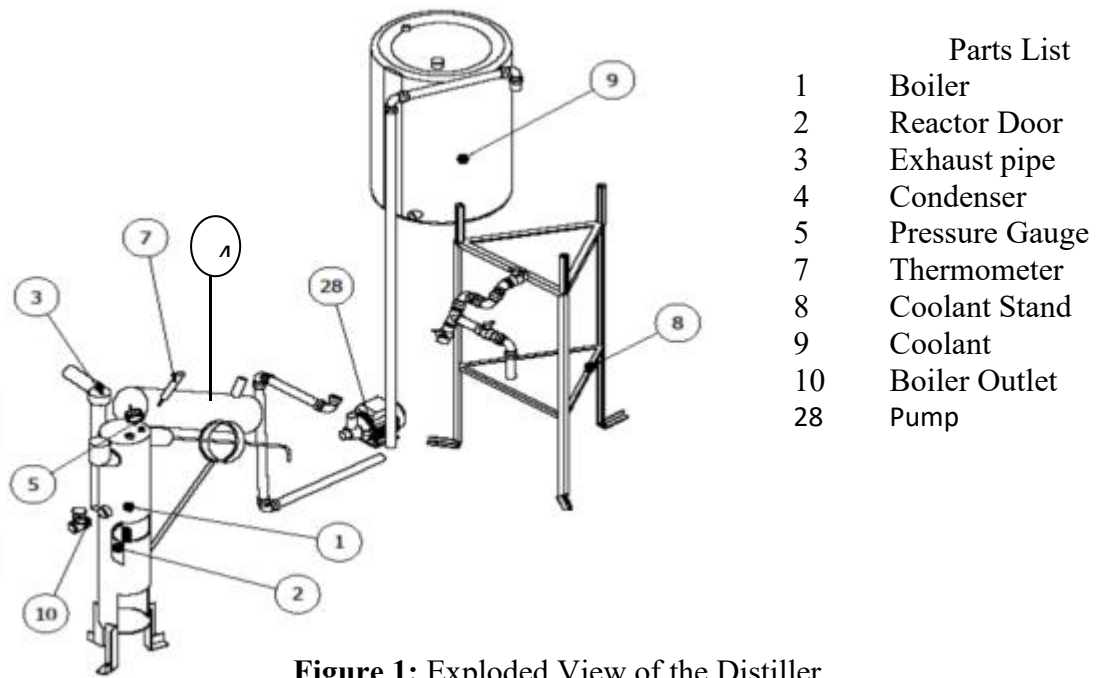


Figure 1: Exploded View of the Distiller



Figure 2: Isomeric View of the Distiller

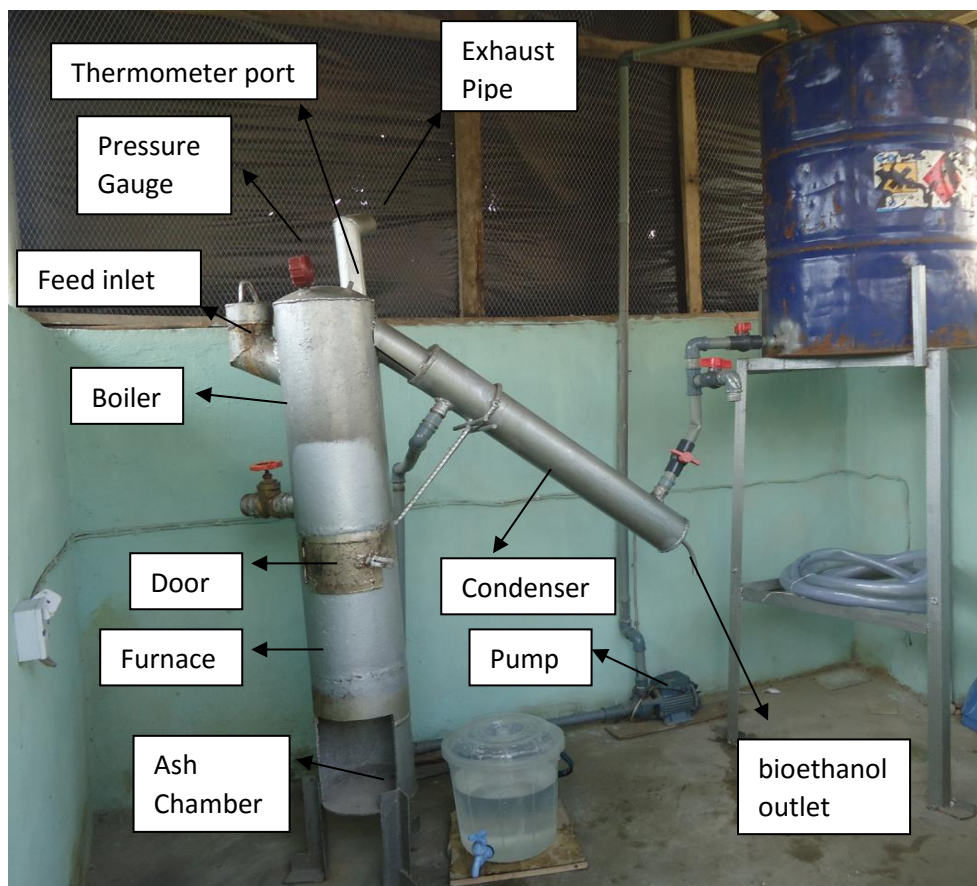


Figure 3: Pictorial View of the Fabricated Distiller

2.7 Performance Evaluation

Twenty Liters of feed at 30 °C prepared from waste palm bunch was fed into the boiler and the reactor charged with locally sourced charcoal. Boiler feed is 1/2 capacity of the boiler in order to accommodate vapour as recommended by Boiling and Suarez (2001). Coolant at ambient temperature of 27 °C was allowed into the condenser at 2.1632×10^{-4} m/s. The distiller follows the principle of producing heat in complete combustion with stoichiometric air requirement of 9.98 kg/kg of charcoal just enough to convert the fuel to ash. The fuel was ignited from the top of the reactor. Air flows in at the bottom while exhaust gas leaves at the top. Sufficient ambient air to burn the fuel and distribute hot air was naturally aspirated into the reactor at airflow rate of 14.335 m³/h and superficial air velocity of 0.1047 m/s. This results to mass flow rate of hot air as 0.102 kg/s. The fuel ignition improved towards complete combustion. Combustion zone moved down the reactor at 5.072×10^{-5} (m/s) in a batch mode as charcoal converts to ashes. The reactor generated heat upwards which is directly transferred to the boiler through a heat surface area of 0.038 m², where it acts as the vaporization heat for bioethanol. At this point bioethanol vaporizes above the feed and flows via the delivery pipes across the entire condenser length of 0.88 m and total heat transfer surface area of 0.0551 m². It condenses within the length of the condenser as it loses heat to the circulating coolant. The bioethanol then drops out and was collected as a pure liquid at 28.3 °C in a graduated glass container while coolant outlet temperature was 40 °C. This type of direct heated device is often referred to as an alambic style still (Kris, 2004).

3.0 Result and Discussion

Figure 4 illustrates bioethanol fuel yield from distillation which is the distillate collected with time.

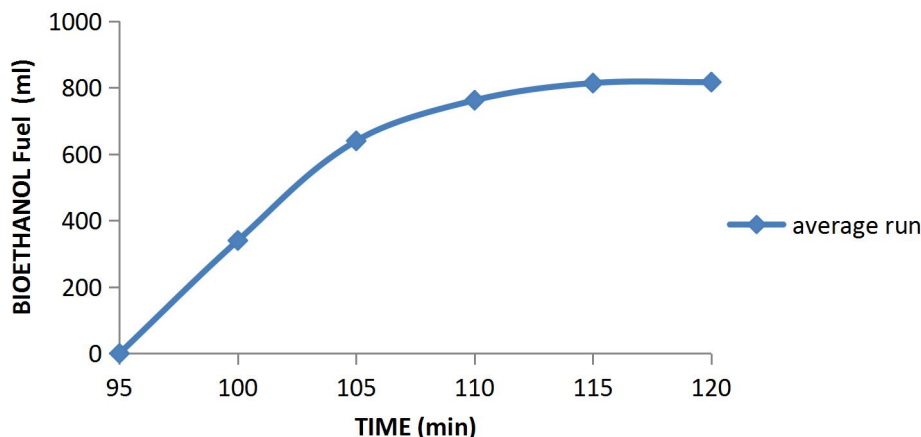


Figure 4: Bioethanol Fuel Yield from Distillation

From Figure 4, it was observed that it took 95 min to get the feed to the boiling point of bioethanol. This boiling time corresponded with the observed temperature and vapour pressure of 96 °C and 2.81 bar respectively. Bioethanol separation from water is initiated at this point. Vapors with a greater concentration of bioethanol formed above the feed (Mathewson, 1980). Figure 4 also shows a progressive increase in yield of bioethanol from 95 min to a maximum of 817 ml at 115 min after which its yield became constant. This means that bioethanol yield stopped at 115 min from the boiling point. The progressive level of bioethanol yield with time to the observed maximum yield prior to the eventual gradual decrease to no yield indicated that bioethanol yield was well regulated by the distiller (Olaye, 2011). Total bioethanol fuel distilled after 20 min was estimated at 817 ml resulting to 2451 ml/h of distillation. This is positive compared to 4.25 L obtained in 1½ h by Olaye (2011) with a reflux column distillation unit. Figure 5 illustrates distillation rate with time.

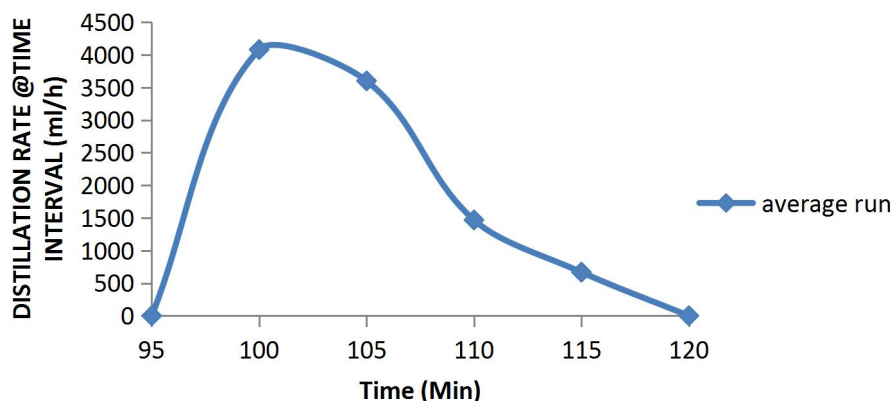


Figure 5: Distillation Rate with Time

It can be deduced from Figure 5 that highest yield rate of bioethanol at interval time was observed at 5 min from the boiling point. Distillation temperature was more stable within this period, suggesting bioethanol molecules having the lowest binding energy with water molecules evaporated at this point (Ophardt, 2003). Production rate depicts how speedy the process was (Will, 2018), which in this case could depend on heat supply and molecules bonding strength

(sudheer 2013; Smith, 1995; Ophardt, 2003). This observation indicated that constant and sufficient heat source was supplied by the machine resulting to avoidance of regression in the process (Olaoye, 2011). Highest yield rate of bioethanol at interval time decreased from 4080 ml/h at 100 min to 668 ml/h at 115 min. Figure 6 illustrates distillation productivity with time.

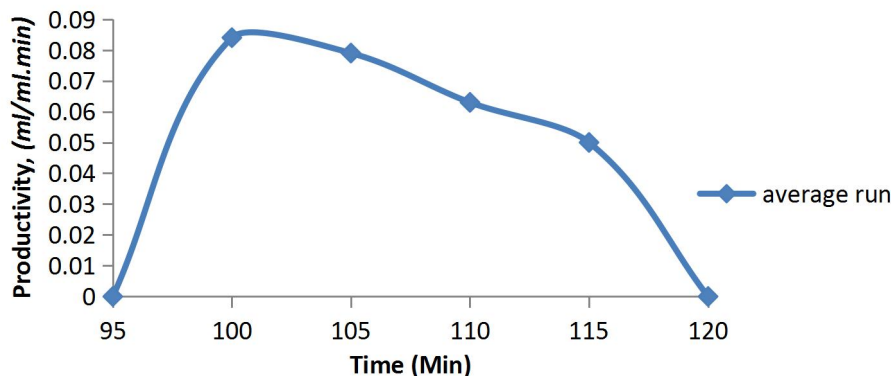


Figure 6: Distillation Productivity with Time

From Figure 6, it was observed that maximum productivity of 0.084 ml/ml.min was attained at 10 min which corresponded to the time of highest distillation rate, and decreased with time within a temperature range. This indicated that the distiller showed reasonable consistency in its operation. It could suggest that, distillation may be seen as a removal process from the boiler of which the material being removed decreases with time at a temperature or within a temperature range. Figure 7 illustrates distillation efficiency with time.

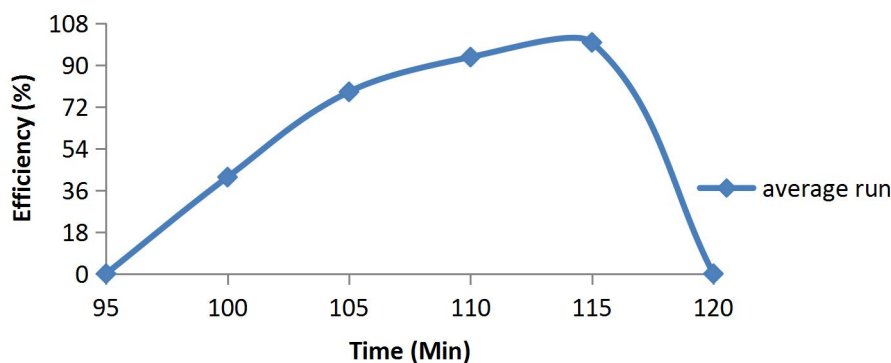


Figure 7: Distillation Efficiency with Time

Figure 7 shows that distillation efficiency increased with time to a maximum of 99.798 % at 115 min. It indicates that the distiller did a quality work though it has small feed capacity, thereby encouraging its adoption and improvement to a larger scale. Distillation process is predicated on the principle of conservation of matter which says that matter can neither be created nor destroyed (Matherson, 1980). Rate of distillation of ethanol is influenced by the ratio of substrate to the ethanol content of the substrate (Olaoye, 2011). Bioethanol yield in liters per volume of feed used is 0.041 (L L⁻¹). This shows that bioethanol concentration was low compared to the volume of the feed. Notwithstanding, this is higher than 0.033 (L L⁻¹) reported by Olaoye (2011). Increasing the bioethanol concentration in the feed before distillation will increase productivity as well as reducing the production costs considerably (Julian et al., 2011). The distilled

bioethanol may not be pure as it may still contain some water and can be further dried in a Rotavapor. Table 1, presents the distiller performance data.

Table 1: Distiller Performance Data

Parameter	Design	Observed	Eqn.
fuel Weight (kg)	1.67	2.2	8
Boiling point (°C)	99.6	95	3
Total operating time (min)	60	115	13
Fuel consumption rate (kg/h)	1.67	1.83	9
Specific gasification rate (kg/hm ²)	80	87.372	12, 13
Combustion zone velocity(m/s)	9.72 E ⁻⁵	5.072 E ⁻⁵	10
Reactor Power input (kW)	8.95	12.2	6
Thermal efficiency (%)	75	55	5
Bioethanol yield (ml)	815.67	817	(Lab)
Distillation Temperature (°C)	99.6	95 - 98	3
Vapor pressure (bar)	3.2	2.81 – 3.01	4
Feed inlet / Distillate outlet temperature (°C)	27 / 27	30 / 28.3	-

Experimental data presented in Table 1 showed that the combustion zone velocity was actually found to be 5.072×10^{-5} (m/s) against 9.72×10^{-5} (m/s) expected. Apart from possibility of absorbing moisture from the environment and fluctuation in natural air flow, this may be due to charcoal porosity and packing in the reactor which influences pressure draft in terms of air flow channel across the fuel bed (Klavina et al., 2014; Joseph and Oliver, 2016). However, all charcoal was reduced to ash. This confirms that complete combustion and good distiller performance was achieved (Bello et al., 2015). Thermal efficiency has been shown to depend more on equipment than fuel selection (Baldwin, 1987; Agyei, 2014). Inefficiencies include incomplete combustion. Also, smoke emission was clear of soot and foul odor was not observed during the process. This confirms good quality of the charcoal specie and sufficient air supply into the fuel column during firing (Bello et al., 2015; Belonio, 2005). The operation was stopped at 120 min and reactor consumed 2.2 kg charcoal at the rate of 1.83 kg/h. But total operating time to consume charcoal observed was 115 min which is 55 min more than expected by the design. The extra 0.527 kg charcoal and time observed may account for the heat used in heating up the boiler material and a lower calorific due to less quantity of acacia charcoal (Abolagba and Nuntah, 2012; Tarig and Osman, 2012). Observed thermal efficiency is 55 % with 12.2 kW power input while design values are 75 % with 8.95 kW respectively. These suggest that the purchased charcoal is having a lower calorific value than the design expected, showing that it contains less quantity of acacia specie (Ijagbemi et al., 2014). Boiling temperature of the bioethanol was observed to be a range than a point, taking place at temperature and vapor pressure range of 96 – 98 °C and 2.81 – 3.01 bars as indicated by the thermometer and pressure gauge respectively from 95 minutes.

4.0 Conclusion

A biofuel distiller of 20 L feed capacity that operates on solid fuel was designed; fabricated and successfully used to distill bioethanol fuel from a 20 L feed. The distiller consists of a 40 L volume

boiler unit integrated to the combustion chamber as a cylindrical column; and a counter current cylindrical condenser of length, tube / shell internal diameter of 88 cm, 0.0191 / 0.15 m, inclined at 45°. The reactor is a Top Lit Updraft (T-LUD) type fired with charcoal of moderate lump. Heat generated upwards was directly transferred to the boiler where it acts as the vaporization heat. The distiller recorded combustion efficiency of 55 % operating on Charcoal. Feed fed to the boiler at 27 °C was heated to boiling point of bioethanol at 95 min while 817 ml distillate was collected in 20 min at 28.3 °C. Boiling temperature of the distillate was observed to be a range than a point of which the thermometer and pressure gauge recorded temperature and vapor pressure range of 96 – 98 °C and 2.81 – 3.01 bars respectively from 95 minutes. The distiller is environment friendly and economically viable.

References

- Abolagba, OJ. and Nuntah, JN. 2012. Effects of oil bean wood charcoal as energy source and two treatments on the characteristics of smoked lean and fatty fish species, using full drum smoker. *Nigerian Journal of Agriculture, Food and Environment*. 8(4): 43-45.
- Adzimah, K. and Seckley, E. 2009. Improvement on the design of a cabinet grain dryer. *America Journal of Engineering and Applied Science*, 2: 217-228.
- Agyei A., Tawiah PO. and Nyarko F. 2014. Efficient Charcoal Stoves: Enhancing their Benefits to a Developing Country using an Improved Design Approach. *International Journal of Engineering Trends and Technology (IJETT)*, 15(2): 94 – 100.
- Antonia, VH., Timothy, EL., Jennifer, IE. and Daniel, MK. 2001. Renewable energy sources: a viable choice. *Journal of Environment*, 43(10): 1 – 17.
- Baldwin, SF. 1987. Biomass stoves: Engineering design, development, and dissemination. Center for Energy and Environmental Studies. Princeton University New Jersey, USA. Publish by VITA, USA. November. pp. 382.
- Baqi, MA., Ahiduzzuman, M. and Rahman, M. 2008. Experiences in installation and operation of energy efficient rice parboiling system. *Short Course on Energy Efficiency, Bangladesh Rice Research Institute (BRRI) Dhaka*, pp. 108-124.
- Bello, RS., Adegbulugbe, TA. and Onilude, MA. 2015. Characterization of three conventional cookstoves in South Eastern Nigeria. *Agricultural Engineering International: CIGR e-Journal*, 17(2):122 – 129.
- Belonio, AT., 2005. Rice husk gas stove handbook. Appropriate Technology Center, Department of Agricultural Engineering and Environmental Management, College of Agriculture, Central Philippine University Iloilo City, Philippines, I, pp. 155.
- Bolling, C. and Suarez, N. 2001. Brazilian sugar industry: recent developments, special article, Sugar and sweetener situation and outlook. Economic Research Service, USDA. September 2001. <http://www.usda.gov/briefing/Brazil/braziliansugar.pdf>. Accessed 9th Feb. 2017.
- Caputi, A., Ueda, M. and Brown, T. 1968. Spectrophotometric determination of ethanol in wine. *American Journal of Enology Viticulture*, 19: 160 – 165.
- Collier, JG. 1982. Convective boiling and condensation. 2nd edition, McGraw Hill, New York, USA.

Congcong, C., Hou-min, C., Zhijan, L., Hasan, J. and Zeng, Z. (2013). Sugars Analysis of Hydrolyzate: A Method for Rapid Determination of Sugars in Lignocellulose Prehydrolyzate. *BioResources*, 8(1): 172 – 181.

Demirbas, A. 2006. Global biofuel strategies. *Energy Education Science Technology*, 17: 27- 63.

Eke, AB. 1991. Experimental performance evaluation of laboratory and field solar and hybrid crop dryer. MSc. Thesis, Department of Agricultural Engineering ABU Zaria Nigeria.

Emerhi, E. 2011. Physical and combustion properties of briquettes produced from sawdust of three hardwood species and different organic binders. *Advance Applied Science Research*, 6: 236 - 246.

ET. 2016. Theoretical air for combustion. *Engineering Toolbox (ET)*, www.engineeringtoolbox.com Accessed 12th Feb. 2017.

FAO 1985. Industrial charcoal making. Food and Agricultural Organization of the United Nations, Rome – Technology and Engineering, 63, pp 133.

Frank, I. and David, D. 2002: Fundamentals of heat and mass transfer. John Wiley and Sons, New York, 5th edition.

Hassan, S., Nor, F., Zainal, Z. and Miskam, M. 2011. Performance and emission characteristics of supercharged biomass producer gas-diesel dual fuel engine. *Journal of Applied Science*, 11: 1606 – 1611.

Iguaz, A. and Vi'rseda, P. 2007. Moisture desorption isotherms of rough rice at high temperatures. *Journal of Food Engineering* 79: 94-802.

Ijagbemi, C., Adepo, S. and Ademola, K. (2014). Evaluation of combustion characteristic of charcoal from different tropical wood species. *International Organization of Scientific Research Journal of Engineering*, 4(4): 50 - 57.

Jim Clark 2005. Non ideal mixture of liquids. www.chemguide.co.uk/physical/phaseeqia/nonideal.html. Accessed 18th June, 2015.

Jones, J. and Dugan, R. 1998. *Engineering thermodynamics*. Published by Prentice Hall India Limited, New Delhi.

Joseph, KK. and Oliver, H. 2016. Experimental evaluation of bulk charcoal pad configuration on evaporative cooling effectiveness. *CIGR Journal*. 18(4):11.

Julia'n, AQ., Luis, ER. and Carlos, AC. 2011. Production of bioethanol from agro industrial residues as feedstocks. Academic Press, Elsevier, USA. 1st Jan., 251 – 285.

Karl, E., Magnus, H., Björn, R., Mats, W. and Roger, W. 2005. Blending of ethanol in gasoline for spark ignition engines. Study performed by Stockholm University, ATRAX AB, Auto emission KEE Consultant AB, and AVL MTC Motor test center AB, Stochholm, Sweden, pp. 133. www.avlmtc.com.

Kays, WM. and Perkins, HC. 1972. Chapter 7. *Handbook of Heat Transfer*. (Rohsenow WM. and Hartnett JP. Eds.). McGraw-Hill Publisher, New York.

Khurmi, R. and Gupta, J. 2006. *Thermal Engineering*, Two colour edition. Chand and Company Limited, New Delhi.

- Kister, H. 1992. *Distillation Design*, illustrated Edition. McGraw-Hill, New York, USA, pp. 710.
- Klavina, K., Cinis, A. and Zandeckis, A. 2014. A study of pressure drop in an experimental low temperature wood chip dryer. *Agronomy Research*, 12(2):511–518.
- Kris, A. 2004. *Artisan Distilling. A guide for small distilleries*. 1st Electronic Edition, Kris Berglund Publishing Inc., Michigan State, East Lansing, USA.
- Leland, MV. 2005. A review of pervaporation for product recovery from biomass fermentation processes. *Journal of Chemical Technology and Biotechnology*. 80:603–629.
- Li, X., Kim, TH. and Nghiem, NP. 2010. bioethanol production from corm stover using aqueous ammonia pretreatment and two-phase simultaneous saccharification and fermentation. *Bioresource Technology*, 101: 5910-5916.
- Mathewson, SW. 1980. *The manual for the home and farm production of alcohol fuel*. Ten Speed Press JA. Diaz Publications, USA.
- NNPC 2005. *Draft Nigerian Bio-fuel Policy and Incentives*. Nigerian National Petroleum Corporation, Lagos, Nigeria.
- Nurul, A., Nasrin, A., Loh, S. and Choo, Y. 2014. Bioethanol production by fermentation of oil palm empty fruit bunches pretreated with combined chemicals. *Journal of Applied Environmental and Biological Sciences*, 4(10): 234 - 242.
- Tongfan, S., Kerry RB. and Aryn ST. 2004. Correlation and prediction of salt effects on vapor–liquid equilibrium in alcohol–water–salt systems. *Advances in Chemistry Series*, 219(2):257 - 264.
- Ophardt, P. (2003). *Chemistry of Hydrogen Bond*. *Journal of Applied Chemistry*, 73: 18 – 24.
- Ojolo, S., Abolarin, S. and Adegbenro, S. 2012. Development of a laboratory scale updraft gasifier. *International Journal of Manufacturing Systems*, 2:21- 42.
- Ojolo, SK, Orisaleye, JJ., Ismail, SO., Abolarin, SM. 2012. Technical potential of biomass energy in nigeria. *Ife Journal of Technology*, 21(2):60 – 65.
- Olaoye, JO. 2011. Design and construction of a reflux column distillation unit for bioethanol production from sugarcane substrate. *Nigerian Journal of Technological Development*, 8 (1): 1 - 13.
- Don, WG. and Robert, HP. 1997. *Perry's Chemical Engineers' Handbook*. McGraw-Hill Incorporation, New York, USA, 8th edition, pp. 2,700.
- Piotr O., Przemyslaw L., Jens H., Anne BT. and Mette HT. 2008. Ethanol production from maize silage as lignocellulosic biomass in anaerobically digested and wet-oxidized manure. *Bioresources Technology*, 99(13):5327 – 5334.
- Rathore, N., Panwar, N. and Vijay, C. 2009. Design and techno economic evaluation of biomass gasifier for industrial thermal applications. *African Journal of Environmental Science and Technology*, 3(1): 006-012.
- Reed, T. B. 1981. *Biomass gasification: Principles and Technology*, Noyes Data Corporation Publishers, Park Ridge, New Jersey, USA, illustrated Edition, pp. 401.

- Rohsenow, WM., Webber, JH. and Ling, AT. 1956. Effect of vapor velocity on laminar and turbulent film condensation. *Transactions of American Society Mechanical Engineering*, 78:1637-1643.
- Sheng, C. and Azevedo, J. 2005. Estimating the higher heating value of biomass fuels from basic analysis data. *Biomass and Bioenergy*, 28(5): 499-507.
- Shyam, P., Amit, S. and Sahoo, P. 2012. Experimental investigation on the performance and emission characteristics of a diesel engine fuelled with ethanol, diesel and jatropha based biodiesel blends. *International Journal of Advances in Engineering and Technology*, 4(2):341 – 353.
- Singh, S. 2008. *Mechanical Engineers Handbook*. Khanna Publishers, New Delhi India.
- Smith, R. 1995. *Chemical process design*. McGraw-Hill, Incorporation, New York, USA, pp. 460.
- Smith, JM., Van Ness, HC. and Abbott, MM. 2001. *Introduction to Chemical Engineering Thermodynamics*, 6th Edition. McGraw-Hill International Edition, Boston, USA, pp. 789.
- Somchart, S., Thanit, S., Adisak, S., Somboon, W. and Boonrueng, S. 2000. Cylconic Rice husk furnace and its application on paddy rice drying. *International Energy Journal*, 1(2): 2 – 9.
- Srinivasa, SG. and Murali, KM. 2016. Performance evaluation of high pressure down draft biomass gasifier for big/gt applications. *International Journal of Engineering Research*, 5: 499 – 505.
- Sudheer, N. 2013. Performance of C.I Engine by using Biodiesel-Mahua Oil. *American Journal of Engineering Research (AJER)*, 2: 22 - 47.
- Tarig, OK. and Osman, TE. 2012. Heat value of four hardwood species from Sudan. *Journal of Forest Products and Industries*, 1(2): 5 - 9.
- Theraja, BL. and Theraja, AK. 2001. *Electrical Technology in S.I Systems of Units*, 4th Edition, Revised. (Tarnekar SG., Khedkar MK. and Sedha RS. Eds.), New Delhi S.Chand and Company Limited Publishers, India, pp. 2,782.
- Will, K. 2018. *Insight markets and economy: Production rate*. Investopedia, Dotdarsh Publishing Family, New York, USA.
- Wusana, AW., Sunu, H., Juli, N. S. and Doyok, P. 2014. Effect of biomass feed size and air flow rate on the pressure drop of gasification reactor. *Journal Teknologi*, 68(3): 7– 12.
- Yong, T., Lee, K., Mohamed, A. and Subhash, B. 2007. Potential of hydrogen from oil palm biomass as a source of renewable energy worldwide. *Energy Policy*, 35(11): 5692-5701.
- Yuelei, Y., Kevin, B. and Dan, Z. 2012. A sustainable ethanol distillation system. *Journal of Sustainability*, 4: 92-105. www.mdpi.com/journal/sustainability
- Yunus, AC. and Afshin, JG. 2015. *Heat and Mass Transfer. Fundamentals and Applications (Sie)*, McGraw Hill Publisher, New York, 5Th Edition.
- Yusoff, S. 2006. Renewable energy from palm oil – Innovation of effective utilization of waste. *Journal of Cleaner Production*, 14: 87- 93.